DEFORMATION FEATURES OF MONO-, POLYCRYSTALLINE AND AMORPHOUS QUARTZ DURING DEPTH-SENSING INDENTATION

D. GRABCO[1,*], O. SHIKIMAKA[1], C. PYRTSAC[2]

[1] Institute of Applied Physics, State University of Moldova, Academy str., 5, Chishinau, MD2028, Republic of Moldova
E-mails: daria.grabco@ifa.usm.md; olga.shikimaka@ifa.usm.md
[2] Technical University of Moldova, Chishinau, MD2004, Republic of Moldova
E-mail: constantin.pirtac@fiz.utm.md
[*] Corresponding author, *E-mail:* grabco@mail.ru

Received June 3, 2025

Abstract. The phenomenon of plastic instability (steps) arising during depth sensing indentation (DSI) measurements of different types of quartz: α-SiO_2, p-SiO_2 and a-SiO_2 is investigated. It is shown that plastic deformation of all types of quartz is characterized by two main mechanisms: shear flow and compaction of the structure. It is suggested that quartz deformation during DSI occurs by a special twinning mechanism, an atomic-rotational type mechanism, with a nanoscopic change in shape, in contrast to conventional (translational-rotational) twinning.

Key words: Quartz of different types: α-SiO_2, p-SiO_2 and a-SiO_2; depth sensing indentation; deformation mechanisms: shear flow, structure compaction, atomic-rotational type of twinning.

DOI: https://doi.org/10.59277/RomJPhys.2026.71.603

1. INTRODUCTION

In recent years, the study of mechanical properties of solids on the micro/nanometer scale has become increasingly active and has expanded its scope of research through the practical application of various classes of materials [1–3]. Systems created on the basis of these materials can combine various mechanical, optical, and electrical functions in devices with micrometer dimensions. It is known that mechanical properties, like many other physical characteristics, largely depend on the structure of the material at the atomic, nano-, and microstructural levels, on the perfection of this structure, and on its modification during the transition of the material dimensions from macro- to micro- and even to nanoscales [4–6]. For this reason, it is necessary to more deeply study the patterns of change in the mechanical parameters of a solid during a radical change in its structure due to volumetric miniaturization or the transition from one real structural form to another: single-crystal → polycrystalline → amorphous.

One of the main modern non-destructive methods for determining the mechanical properties of all kinds of materials is the method of dynamic indentation, depth sensing indentation (DSI) [7, 8]. The determination of the parameters of strength and plasticity is carried out in a very wide range of loads: macro-, micro-, nano- and even picoindentation on special high-precision devices – nanotesters. Thanks to this, many specific patterns of deformation of crystals with different types of bonding have been discovered [9], the indentation size effect (ISE) has been revealed [10], the translational-rotational mechanism of crystal deformation has been established [11], etc.

Another important result of recent years is the discovery of the serration effect (SE) (otherwise known as the "oscillation effect") during indentation of various types of materials [12]. It has been established that the oscillation effect depends on the type of sample: it is most pronounced in single crystals and weakest in glasses. It has been found that the oscillatory effect is most pronounced at low loads and low deformation rates. It has been suggested that the oscillation effect may be associated with elastic-plastic recovery (relaxation) of the material, which occurs throughout the entire indentation process and may indicate the wave nature of the indentation process and the universality of the oscillatory effect in the process of dynamic indentation [13–15].

An equally important achievement is the proof of compaction and volumetric shear flow on materials under the action of high local stress [16–19]. Thus, the authors of the work [16] showed on glasses of different compositions that both possible mechanisms make different contributions depending on the glass composition. It was also established that compaction prevails in glasses with a relatively low atomic packing density, and shear flow is included after compaction is achieved. However, despite the revealed regularities, many questions remain unclear. For example, what deformation mechanisms are involved in the process of creating a hardness imprint in crystals with a complex structure, in which the mobility of individual dislocations is extremely low, or what factors promote the relaxation of internal stresses under the action of a concentrated load, and which ones inhibit it? The study of such questions is of interest for the present work.

Taking into account the above, the task of choosing a material for the study was set in the work, which can have several structural forms under normal conditions, in order to identify the effect of the structure on the mechanical properties. For this purpose, the material quartz (SiO_2) is suitable from several points of view. First of all, quartz under normal conditions can exist in various structural forms: single-crystal, polycrystalline, amorphous, which allows tracking the contribution of the structural form to the change in mechanical parameters, the specificity of deformation, the reaction of the material to the impact of various external factors, such as the magnitude of the applied load, the speed of load application. On the other hand, quartz is a very

important material from a technical point of view, demonstrating an excellent combination of valuable electrical and optical properties with high physical strength and high chemical resistance. Therefore, knowledge of the regularities of quartz deformation is of great practical interest.

2. MATERIALS AND METHODS

Three structural types of quartz were used in the study: monocrystalline (α-SiO_2, monocrystal), polycrystalline (p-SiO_2, polycrystal) and amorphous (a-SiO_2, amorphous). It is known [20] that quartz crystals (SiO_2) belong to the trigonal syngony in the temperature range of 273–873K and to the hexagonal synonymy in the range of – 873–1143K. In α-SiO_2 crystals, which belong to the first class, there is no center of symmetry and a plane of symmetry. Quartz crystals can have twins according to three main laws: Dauphiné, Brazilian, Japanese [21]. The α-SiO_2 single crystals studied in the work had the orientation (0001). The cleavage planes of quartz are the planes of the rhombohedron {1011} and the prism {1010}, but cleavage along them is very difficult. Therefore, the (0001) face was prepared not by cleaving, but by mechanical polishing on a polishing machine, first with Al_2O_3 powder and then with wet CrO_3 powder. Samples of p-SiO_2 and a-SiO_2 were prepared in a similar way.

The mechanical properties were studied using the dynamic indentation method on a Nanotester-PMT-NI-02 device equipped with a Berkovich indenter. The procedure used in the work was to press the indenter in the mode of gradually increasing the load applied to the indenter from 0 to P_{max}, briefly holding under the load, and then gradually decreasing to 0. Continuous record-keeping of the depth of indenter penetration into the material under study allows monitoring the loading/unloading process. During nano- and microindentation tests, the following stages were performed for each sample:

- Loading-unloading process up to maximum loads according to the following scheme: loading – 20 s, holding at maximum load (P_{max}) – 5 s, unloading – 20 s. For each load, 10 imprints were made for α-SiO_2 and p-SiO_2, and 5 imprints for a-SiO_2. The results were calculated as the average value of 10 or 5 tests. The maximum loads varied for five values of P_{max}: 10, 50, 100, 300 and 500 mN.
- All calculations were performed automatically using the device software.
- To study the microstructure of the indentations and its surroundings at higher loads (0.5–5.0) N, a standard PMT-3 device with a Vickers diamond indenter was used.

The microstructure and morphology of the deformed zones were studied using a Nanostation II atomic force microscope (AFM) and optical microscope XJL-101 with digital monitoring. To reveal the fine structure, the crystals were chemically etched in a HF:HBO_3:H_2O solution in a ratio of (1:2:5).

3. RESULTS AND DISCUSSION

Much attention was given to several issues in the work: the dependence of the "serration effect" value on the type of sample, the influence of the indentation load on the manifestation of the "serration effect", the influence of the loading rate on the value of SE, as well as the change in the surface relief around the indentations depending on the type of structure and the magnitude of the load.

Since the samples under study were manufactured by mechanical polishing, chemical etching was used to check the quality of the surface obtained for testing (absence of a work-hardened layer). As an example, Figs. 1a, 1b show the surface view of α-SiO_2 and p-SiO_2 samples after chemical etching, which shows the microstructure without traces of mechanical polishing. After surface inspection, the samples were subjected to additional light polishing to remove the etching pattern used to apply the indentations. Figure 1c shows the surface view and an indentation applied to the a-SiO_2 sample.

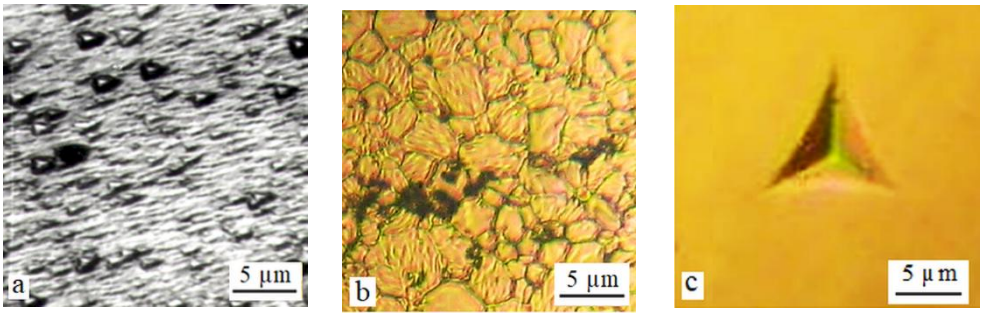

Fig. 1 – Microstructure of quartz after chemical etching (a, b) and after light final polishing (c); a – growth dislocations on the surface of an α-SiO_2 single crystal; b – grain structure of polycrystalline p-SiO_2; c – hardness indentation applied to the finely polished surface of a-SiO_2 amorphous sample, P = 100 mN.

Let us first consider the type of deformation curves obtained at different maximum loads on the studied samples: a – α-SiO_2, b – p-SiO_2 and c – a-SiO_2 (Fig. 2). As expected, based on the literature data [12, 13], the serration effect is visible on all curves and at all the loads used. However, unlike ionic and covalent crystals [14], on all types of quartz the frequency and amplitude of oscillations are rarer and smaller in magnitude.

The serration effect is clearly evident at low loads (curves 1 in Fig. 2) and only weak oscillations are noticeable at higher loads (curves 2–5 in Fig. 2). The effect can be seen much better in Figs. 3–5, which show the deformation curves $P(h)$ for three loads P_{max}= 10, 50 and 500 mN for all types of samples.

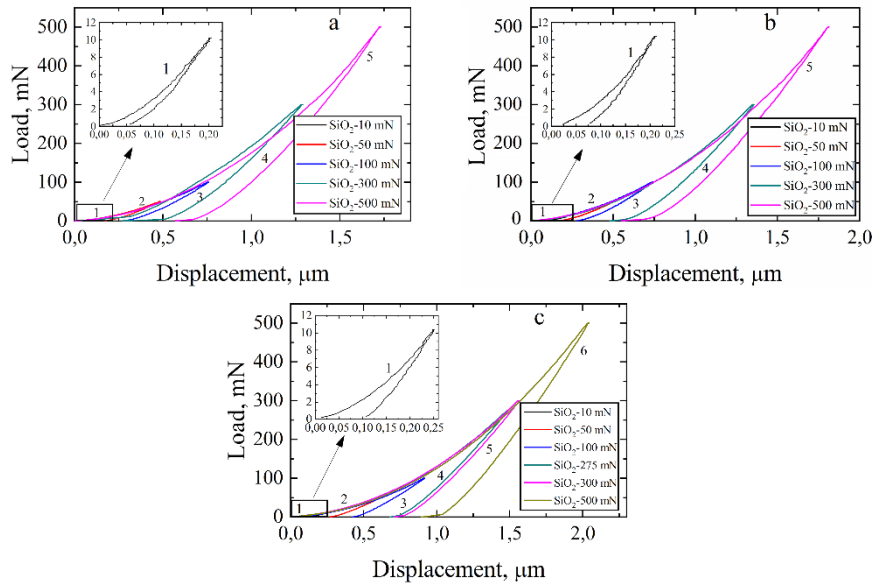

Fig. 2 – Loading–unloading curves $P(h)$: a – α-SiO_2, b – p-SiO_2 and c – a-SiO_2 at various peak loads.

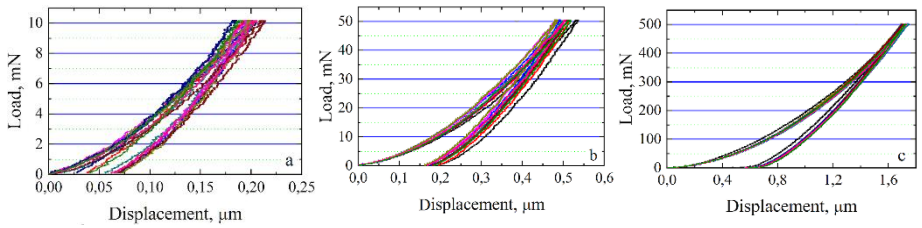

Fig. 3 – α- SiO_2, single crystal. Loading–unloading curves $P(h)$ at P_{max}, mN: a – 10; b – 50; c – 500.

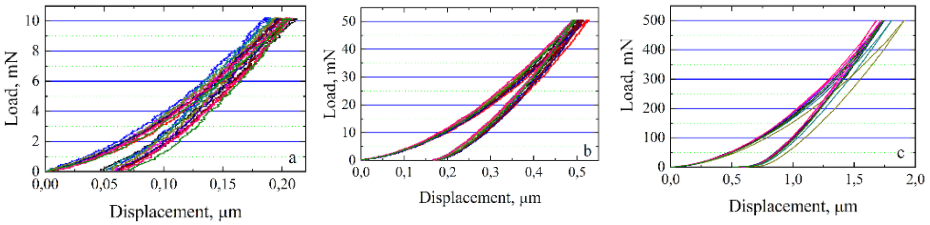

Fig. 4 – p-SiO_2, polycrystal. Loading–unloading curves $P(h)$ at P_{max}, mN: a – 10; b – 50; c – 500.

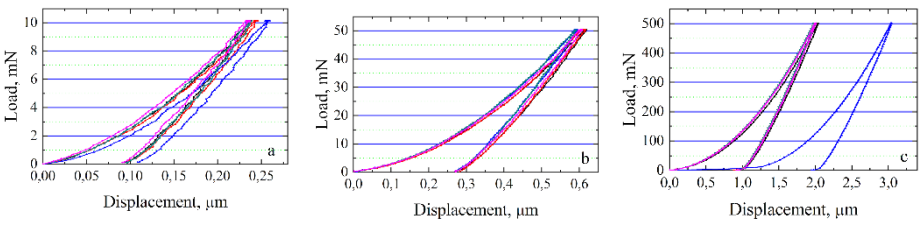

Fig. 5 – a-SiO_2, amorphous. Loading–unloading curves $P(h)$ at P_{max}, mN: a – 10; b – 50; c – 500.

As follows from the given curves, the serration effect is manifested on all three types of samples. Moreover, as was established in works [12-15], the amplitude and frequency of oscillations depend on the value of the maximum applied load, being most clearly manifested at the minimum load. With the growth of P_{max} the effect decreases, the loading/unloading curves become smoother. The amplitude and frequency of oscillations also decrease upon the transition from α-SiO_2, monocrystalline, to p-SiO_2, polycrystalline, then to a-SiO_2, amorphous. However, in general, the serration effect on quartz is manifested to a lesser extent than on crystals of higher crystal system.

The value of the serration effect also depends on the speed of the indentation process. The influence of this factor on the DSI process of quartz is clearly demonstrated by the following figures (Fig. 6), which show two curves for each type of quartz, for the smallest and largest load (P_{max}=10 mN and 500 mN).

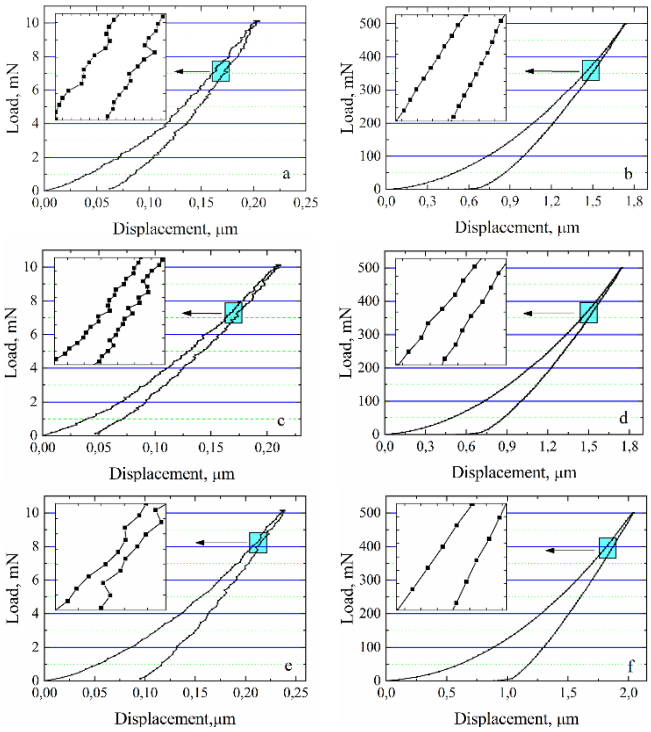

Fig. 6 – α-SiO_2, single crystal (a, b), p-SiO_2, polycrystal (c, d), a-SiO_2, amorphous (e, f). Comparison of deformation curves for small and large loads. Oscillating (wave-like) course of curves at 10 mN (a, c, e) and smooth course at 500 mN (b, d, f).

The presented curves clearly show the effect of decreasing the frequency and amplitude of oscillations on the curves for 500 mN compared to the curves for 10 mN. Since in our experiments the duration of loading and unloading was the same for all loads (20 s), the rate of the indenter penetration process (v_{in}) gradually

increases when passing from the minimum load to the high one. Thus, when passing from P_{max}= 10 mN to P_{max}= 500 mN, the indentation rate increases by two orders of magnitude, from v_{in}= 0.5 mN/s to v_{in}= 25 mN/s. That is, the effect of increasing the homogeneity of the indentation process with increasing load corresponds to the effect of increasing the homogeneity of the process with speed increasing. Therefore, it can be assumed that an increase in the homogeneity of the deformation process with increasing v_{in} may be associated with the limited ability of quartz to relax internal stresses with an increase in the indenter penetration rate.

Thus, the characteristic dependencies obtained in the work correlate with the results of works in which the jagged, wave-like nature of indentation in a wide range of loads and speeds was confirmed on a large spectrum of materials. In works [22, 23] it was shown that with a continuous increase in load during uniaxial deformation, elastic-plastic deformation bands in the form of localized plasticity autowaves are successively formed in the sample. After the passage of primary autowaves, a continuing increase in load causes the activation of new deformation zones. It was also stated that the process of generation and propagation of autowaves is repeated many times during the action of an external load.

It is interesting to draw an analogy between the process of oscillation initiation and propagation during depth sensing indentation with the behavior of a material during uniaxial deformation. It is noted that each act of oscillation initiation and annihilation (otherwise fluctuations or autowaves) during DSI undergoes the same stages that a material goes through during uniaxial deformation, only on a nano- or microscale. To confirm this, Fig. 7 shows a typical stress/strain curve, $\sigma(\varepsilon)$, for uniaxial deformation of materials.

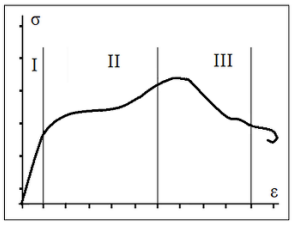

Fig. 7 – Typical curve of σ(ε) (stress/strain) dependence for uniaxial deformation of materials. I – elastic stage; I – strengthening stage; III – softening (plastification) stage.

As was mentioned above, the indenter pressing procedure during DSI was carried out in the mode of gradual increase of the load applied to the indenter from 0 to P_{max} and gradual decrease to 0. Therefore, initially, when the load is applied, elastic compression of the nearby lattice atoms of the deformed sample occurs similar to stage I on the $\sigma(\varepsilon)$ curve (Fig. 7). A subsequent increase in the load forms an elastic-plastic layer near the indenter in the form of stripes or deformation zones of nanoscale size, which resists the increasing load similar to stage II, the strengthening stage. A further increase in the load leads to an increase in the number of localized plasticity defects, their interaction and partial annihilation (similar to stage III, the softening stage). The interaction of newly created defects reconstructs the area of localized plasticity, reducing its elastic resistance, and thereby creates conditions for the activation of new

deformation zones of nano-, submicro- and microscales and an increase in the size of the deformed zone in the vicinity of the indenter. The origin and propagation of new zones of localized plasticity will be repeated many times in jumps during the action of an external concentrated force by analogy with the mechanism considered in [22, 23]. Due to the action of such a deformation mechanism, the indentation curves acquire an oscillatory, jump-like character.

It should be noted that the heterogeneity of the process occurs not only at the loading stage, but also at the unloading one (see Figs. 2–6). The abrupt nature of the deformation is also revealed when studying the microstructure of hardness indentations after complete unloading of the sample. Thus, Fig. 8 shows the view of indentations at P_{max}=500 mN (b, e, h) and profiles in the section at two loads P_{max}=50 and 500 mN (a, d, g, c, f, i) for three types of quartz (α-SiO2, p-SiO2 and a-SiO2), obtained by the AFM method.

The presented figure clearly shows the regularities noted above in the deformation curves (see Figs. 2–6). It follows from Fig. 8 that both the profiles of the indentations and the 3D images demonstrate a finely jagged, wavy appearance.

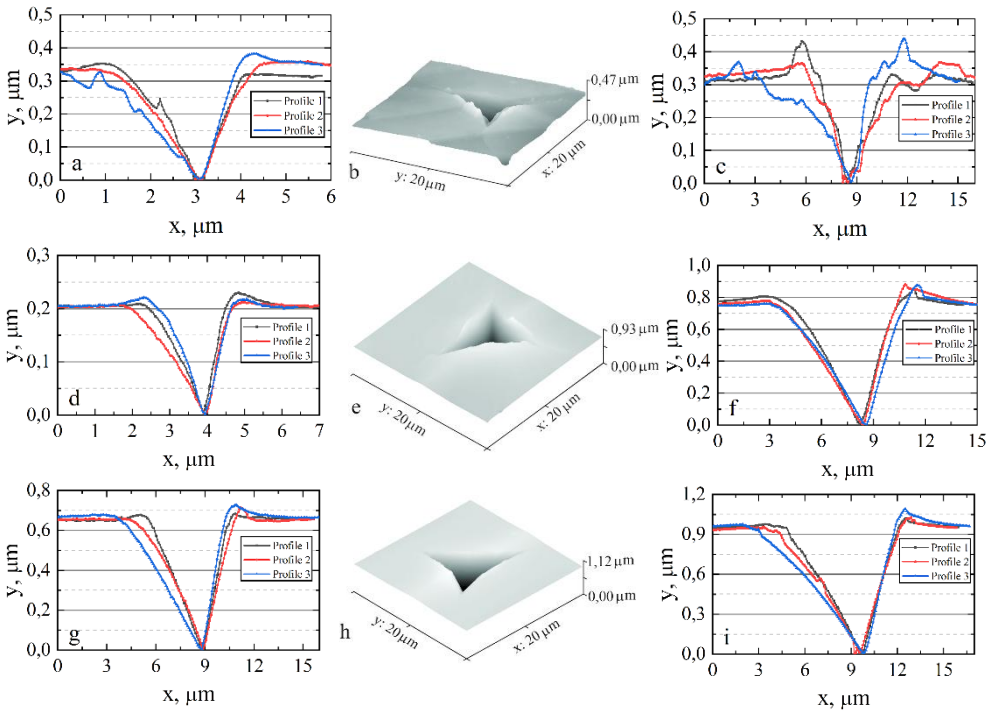

Fig. 8 – AFM view of indentations at P_{max}=500 mN (b, e, h) and cross-sectional profiles at two loads: P_{max}= 50 and 500 mN (a, d, g, c, f, i) for three types of quartz: α-SiO2 (a, b, c); p-SiO2 (d, e, f); a-SiO2 (g, h, i).

This indicates that the unloading process is not smooth, but occurs in continuous light jerks. In addition, large waves appear on the profiles of the α-SiO2 indentations after complete unloading. This may be due to the uneven elastic recovery of the indentation [24, pp. 22–25]. Elastic recovery of the deformed area compressed by the indenter leads to the formation of pile-ups around the indentations. As follows from Fig. 8, their formation again obeys the same regularity: the maximum pile-ups are formed near α-SiO2 and decrease upon transition to p-SiO2 and a-SiO2.

The analysis of the indentation profiles using atomic force microscopy also provided very important information regarding the mechanism of the indentation formation (Fig. 9). It follows from the figure that the pile-ups decrease with the transition in the series from monocrystalline quartz to polycrystalline and then to that of amorphous. This indicates that, accordingly, there is an increasing compaction of the material in the region adjacent to the indenter. Having reached certain critical values, the resulting stresses can suddenly relax, causing rotation of individual nano- and microassemblies of the material and creating a denser packing.

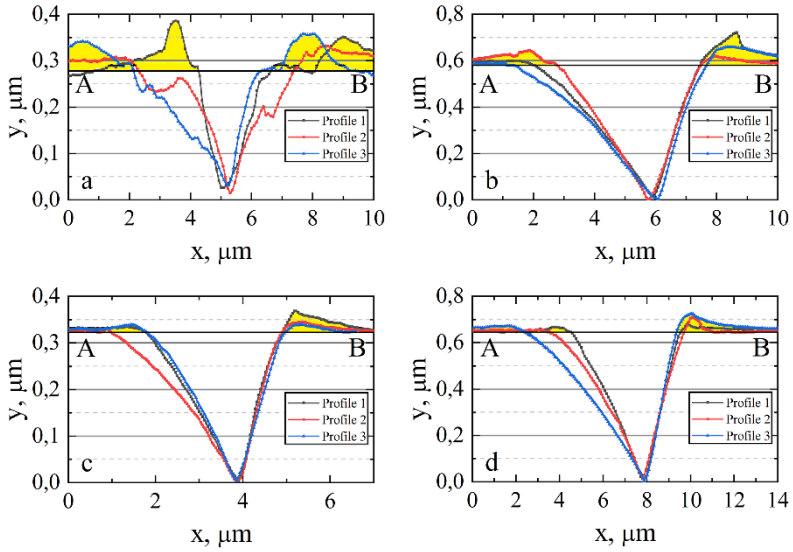

Fig. 9 – AFM. Profiles of indentations in the section under two loads: P = 300 mN (a,b) and 100 mN (c,d) for three types of quartz: α-SiO_2 (a); p-SiO_2 (b,c); a-SiO_2 (d). AB is the level of undeformed surface of the sample.

In works [16–19] it is shown that compaction is a sharp compression of the substance into a more closely packed structure and is a transformation of displacement. The lower the density of the atomic packing of sample, the greater the magnitude of the volume shrinkage. The authors [17] estimated that in the case of amorphous silica a-SiO_2, compaction is ~80% of the indentation volume, which is in good agreement with our results.

As indicated in previous studies [20, 21], the mechanism responsible for the compaction of the structure may be a special twinning mechanism called "shape-independent twinning", in contrast to conventional (translational-rotational) twinning. These two types of twinning differ significantly in the mechanism of twinning at the atomic level. Conventional twinning with a microscopic shape change occurs due to formation of twinning dislocations, while twinning by the second mechanism, with a nanoscopic shape change, is a deformation due to atomic displacements.

When speaking about "twinning without shape change", we mean the absence of macro- or microscopic shape change (similar to twinning of calcite or bismuth) [21, 24, 25], but not absolute preservation of the steadfastness of the crystal shape. In the works [26, 27] it was possible for the first time to identify submicroscopic and nano sized deformations in the vicinity of indentation, occurring according to a special plasticity mechanism, the atomic-rotational type mechanism, with submicro- and nanoscopic shape change. Figure 10 shows the areas of plastic rotation of quartz around the indentations applied under a load of P = 2.0 N. The images clearly show areas of reorientation in the vicinity of the indentations with a regular rotation of the crystal lattice by an angle of 60° or 180°, similar to those described in [21, 26, 27].

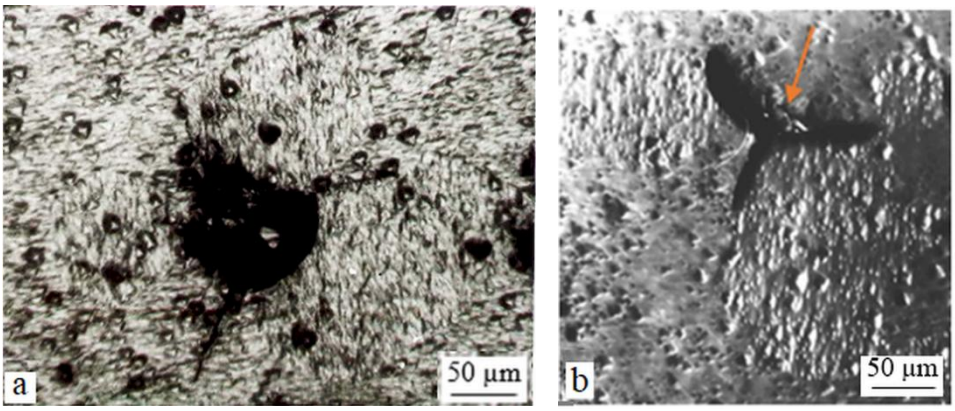

Fig. 10 – Deformation zones around the indentations on the SiO_2 crystal, P = 2.0 N. T_{def} = 800K: a – view of the surface microstructure in the vicinity of indentation after chemical etching; b – view of the surface microstructure after polishing a 1.0 μm layer and etching. The arrow indicates the location of the indentation.

As follows from Fig. 10, the reoriented areas extend over large distances from the place of application of the load (from the indentations) and have an arbitrary border. Most often, twins have an oval-oblong or round shape, however, there are also rectilinear ones and areas without a clear border, with zigzag boundaries. Consequently, it can be considered that, due to the low symmetry and the associated extremely low mobility of dislocations, for the dissipation of high

internal stresses arising under the action of the indenter, the SiO_2 crystal uses a new mechanism, different from the widely known one, rotational twinning, which is characterized by a high-speed process. In accordance with [20, 21], the transfer of atoms from a normal position to a twin position occurs almost simultaneously for a huge number of atoms, which ensures a high speed of the process.

The data accumulated in the work allow us to propose the following evolution of the DSI process. Throughout the entire period of the indenter penetration, the deformation process is accompanied by another synchronous reverse process, leading to the relaxation of the defect structure formed in the material under the action of the load. As a result of the appearance of defect structure, the internal energy in the deformation zone increases sharply, therefore, the atomic structure of the material from the very beginning of the indenter deepening process is reconstructed in such a way as to minimize the internal energy of the sample. Owing to internal displacements of atoms, various effects are observed on the $P(h)$ curves, such as "serration", "pop-in", "pop-out", the formation of "pile-ups" nearby the indenter, as well as compaction of the material in the area under the indentation. The formed defect structure begins to relax even more intensively when the maximum value of the load P_{max} is reached and reduced to complete unloading, which leads to partial restoration of the indentation depth (unloading stage on the $P(h)$ curves). After the indenter is completely removed from the sample, the defect structure continues to restore for some period of time, forming bends on the sides of the residual indentation, the largest ones on the α-SiO_2 indentation profiles. This leads to displacement of the material to the surface and the formation of "pile-ups".

Along with the process of material displacement to the surface in the form of piles, another, opposite process takes place in the sample, the compaction of the material in the area under the indentation. This process is a sharp compression of the substance into a more densely packed structure and is a displacement transformation. A lower atomic packing density of the sample contributes to a greater volume shrinkage, and therefore manifests itself more clearly in the transition from α-SiO_2 to p-SiO_2, then to a-SiO_2. Compression of the structure occurs according to a special mechanism of plasticity, a mechanism of the atomic-rotational type, with submicro- and nanoscopic change in shape. Compaction of the plastic zone in the neighborhood of indentation occurs according to the twinning mechanism. During rotational twinning of quartz, twins arise according to the Dauphine law, *i.e*. twins of rotation. The angle of rotation in this case can be equal to 60° or 180°.

Thus, based on the results obtained in the work, as well as literary data, it can be concluded that depth sensing indentation of quartz with mono-, poly- and amorphous structure is a complex, multi-level process that includes various mechanisms of elastic-plastic mass transfer in the region of maximum tangential stresses when applying a concentrated load and, in particular, during nano-microindentation.

4. CONCLUSIONS

The paper studies the deformation features of mono-, polycrystalline and amorphous quartz under depth-sensing indentation in the load range P_{max}=10–500 mN. It was found that the serration effect is observed on all deformation curves and under all applied loads. The effect depends on the value of the maximum applied load, being most pronounced under the minimum load. With increasing P_{max}, the effect decreases, and the loading/unloading curves become smoother. The amplitude and frequency of oscillations also decrease when moving from α-SiO_2 to p-SiO_2, then to a-SiO_2. However, in general, the serration effect on quartz is less pronounced than on crystals of higher syngonies.

Due to internal displacements of atoms during DSI, pile-ups are formed on the surface around the indentations and the material is compacted in the bulk near the indentation. Direct evidence for compaction and shear flow was obtained using atomic force microscopy and microstructure analysis of indentations on samples subjected to DSI and local concentrated loading. Both mechanisms contribute to the material transport to a greater or lesser extent depending on the quartz type. Compaction predominates in samples with lower atomic packing density (p-SiO_2 and a-SiO_2), while shear flow is more active in denser α-SiO_2. As a result, the shear flow leads to accumulation of the substance near the indentation in the form of pile-ups, while compaction leaves a well-defined indentation surrounded by a slightly distorted flat surface. Modification of the structure occurs by a special mechanism of plasticity, a mechanism of the atomic-rotational type, with submicro- and nanoscopic change in shape. Compaction of the plastic zone in the vicinity of the indentation occurs by the twinning mechanism. It is shown that during rotational twinning of quartz, twins arise according to the Dauphiné law, *i.e.* rotation twins.

Acknowledgements. This study was supported by the research Subprogram **011201** of the Institute of Applied Physics, State University of Moldova, funded by the Ministry of Education and Scientific Research of Moldova Republic.

REFERENCES

1. S.P. Moylan, S. Kompella, S. Chandrasekar, and T.N. Farris, Tribology Series **39**, 895–903 (2001). https://doi.org/10.1016/S0167-8922(01)80169-3
2. J. Shaocheng, G. Qi, and X. Bin, J. Mater. Sci. **41**, 1757–1768 (2006). DOI: 10.1007/s10853-006-2871-93.
3. Z. Xue, Z. Zhu., D. Zhu, T. Li., and Ch. Yang, J. Mater. Sci. **58**, 3752–3767 (2023). https://doi.org/10.1007/s10853-023-08234-8.
4. Yu. I. Golovin, Phys. Status Solidi **50** (12), 2205-2236 (2008). DOI: 10.1134/S1063783408120019.
5. D.I. Brinkevich, N.V. Vabishchevich, S.A.Vabishchevich, V.S. Prosolovich, and Yu.N. Yankovskii, J. Surf. Investig. **7**, 1217–1220 (2013). https://doi.org/10.1134/S1027451013060256.

6. Z. Chao, H. Jianhua, L. Ainong, H. Shangyu, L. Hanxing, C. Gang, L. Anqi, Z. Zhang, L. Bei, and W. Zhengzhi. J. Mater. Sci. & Chem. Eng. **6** (4), 57–64 (2018). DOI: 10.4236/msce.2018.64008.
7. W.C. Oliver and G.M. Pharr, J. Mater. Res. **7**, 1564–1583 (1992). DOI: *10.1557/jmr.1992.1564*.
8. H. Hu and Zh. Hongwei, Sci. Adv. Mater. **6**, 875–889 (2014). DOI: 10.1166/sam.2014.1868.
9. D. Grabco, C. Pyrtsac, and O. Shikimaka, Phys. Status Solidi **62** (8), 1386–1393 (2020). DOI: 10.1134/S106378342008017X.
10. Z. Zong and W. Soboyejo, MSEA **404**, 281–290 (2005). DOI: 10.1016/j.msea.2005.05.075.
11. D. Grabco, O. Shikimaka, and E. Harea, J. Phys. D: Appl. Phys. **41**, 074016 (2008). DOI: 10.1088/0022-3727/41/7/074016.
12. N.Q. Chinh, J. Gubicza, Zs. Kova´cs, and J. Lendvai, J. Mater. Res. **19** (1), 31–45 (2004). DOI: 10.1557/jmr.2004.0004.
13. A. Dey, R. Chakraborty, and A.K. Mukhopadhyay, Appl. Glass Sci. **2** (2), 144–155 (2011). DOI: 10.1111/j.2041-1294.2011.00046.x.
14. D. Grabco, C. Pyrtsac, and O. Shikimaka, ICNBME-2023, IFMBE Proceedings **91,** 1–10 (2024). https://doi.org/10.1007/978-3-031-42775-6_11.
15. D. Grabco, O. Shikimaka, C. Pyrtsac, D. Topal, D. Vilotic, M. Vilotic, and S. Alexandrov, Metals **13**, 1278–1291 (2023). DOI.org/10.3390/met13071278.
16. T. Rouxel, H. Ji H, JP Guin, F. Augereau, and B. Rufflé, J. Appl. Phys. **107**, 094903 (2010). DOI: 10.1063/1.3407559.
17. D. Vandembroucq, Th. Deschamps, C. Coussa, A. Perriot, E. Barthel, B. Champagnon, and C. Martinet, J. Phys.: Condens. Matter. **20**, 485221 (2008). DOI: 10.1088/0953-8984/20/48/485221.
18. S. Yoshida, H. Sawasato, T. Sugawara, Y. Miura, and J. Matsuoka, J. Mater. Res. **25** (11), 2203–2211 (2010). DOI: https://doi.org/10.1557/jmr.2010.0287.
19. V. Keryvin, S. Gicquel, L. Charleux, J. Guin, M. Nivard, and J.-Ch. Sangleboeuf, Key Eng. Mater. **606**, 53–60 (2014). DOI: 10.4028/www.scientific.net/KEM.606.53.
20. M.P. Shaskolskaya, *Crystallography* (in Russian), Higher School, Moscow, 1976.
21. M.V. Klassen-Hekliudova, *Mechanical twinning of crystals* (in Russian), Moscow, 1960.
22. L.B. Zuev, S.A. Barannikova, N.B. Zarikovskaya, and I. Zhykov. Phys. Status Solidi **43**(8), 1423–1428 (2001). DOI: 10.1134/1.1395088
23. V.I. Danilov, L.B. Zuev, V.V. Gorbatenko, L.V. Danilova, and D.V. Orlova. JTF, **91** (2), 267–274 (2021). DOI: 10.21883/JTF.2021.02.50361.35-20.
24. Iu.S. Boyarskaya, D.Z. Grabco, and M.S. Kats, *Physics of Microindentation Processes* (in Russian), Ştiinţa, Chişinău, 1996.
25. D.Z. Grabco, Iu.S. Boyarskaya, and M.P. Dyntu, *Mechanical properties of bismuth type Semimetal* (in Russian), Ştiinţa, Chişinău, 1982.
26. O. Shikimaka, Abstract at the VI National Colloquium, FTMCA-6, Iaşi, Romania, pp. 87–88, 2000.
27. O.A. Shikimaka and D.Z. Grabco, Proceedings of the Conference “Actual Problems of Strength” (in Russian), Vitebsk, pp. 216–224, 2004.